

Optical Absorption due to Free Holes in Germanium: A Comparison of Theory and Experiment

J. B. ARTHUR, A. C. BAYNHAM, W. FAWCETT, AND E. G. S. PAIGE
Royal Radar Establishment, Malvern, Worcestershire, England

(Received 13 June 1966)

The absorption due to direct inter-valence-band transitions of free holes in germanium has been investigated. A comparison is made between the computed and experimental change of absorption induced by a small increment of lattice temperature. The theory is based on the exact treatment of the $\mathbf{k}\cdot\mathbf{p}$ interaction between bands, and is extended here to include evaluation of the optical matrix elements. A method of computing the absorption is described in which the full complexity of the band structure is incorporated. The results of the calculation are fitted to the experimental data by varying the parameters within the limits provided by known band-structure data. A good fit is obtained, but discrepancies exist which are outside experimental error.

I. INTRODUCTION

THE high-energy extremum of the valence band near $k=0$ in germanium consists of three doubly degenerate bands. Two of these, the heavy-mass and the light-mass bands, are degenerate at $k=0$, while the third is depressed to lower energy by spin-orbit interaction. In material where the impurity content¹ is less than about 10^{16} cm⁻³, the optical absorption associated with free holes arises primarily from direct transitions between the bands, and though when the photon energy is considerably less than the spin-orbit splitting energy, phonon-assisted transitions can become important. The direct transitions give rise to structure in the absorption,^{2,3} a peak above the spin-orbit splitting energy (0.295 eV) due to (1-3) transitions,⁴ a peak below, but close to, the spin-orbit splitting energy due to (2-3) transitions, and a shoulder at about 0.2 eV due to (1-2) transitions.^{5,6} With the exception of the peak due to the (2-3) transition, which is not observed because of the low temperature, these features can be seen if reference is made to Fig. 4 below, which shows the absorption as a function of photon energy (solid curve) at 77°K. More detailed structure associated with the inter-valence-band transitions appears in the spectrum of the change in absorption produced by a small increment in lattice temperature^{7,8} (see Fig. 3 below). We shall refer to this as the "differential" absorption spectrum. The main objective of this paper is to present a comparison between a computation of the differential absorption due to direct transitions, based on the recent theory of the valence-band structure given by Fawcett,⁹ and experimental results.

Previous calculations of the optical absorption have been based on second-order $\mathbf{k}\cdot\mathbf{p}$ perturbation theory. Kahn⁵ simplified his calculation by assuming that the spin-orbit splitting energy was large compared with the energy of the holes. In this approximation, band 3 is effectively decoupled from bands 1 and 2 and all bands are parabolic. Though this calculation reproduced some of the features observed in the optical absorption, the calculated contribution from (1-2) transitions became unrealistically large at high lattice temperatures and was predicted to mask the observed structure from (1-3) and (2-3) transitions. Kane⁶ removed the assumption of large spin-orbit splitting energy and was able to obtain qualitative agreement with experimental data over a range of lattice temperatures.

In Fawcett's⁹ theory of the valence-band structure, $\mathbf{k}\cdot\mathbf{p}$ interactions between the valence band and the nearest three conduction bands have been treated exactly rather than by perturbation theory. This treatment leads to differences in the predicted band structure, notably a less energy-dependent band 3, which are such as to suggest that the agreement between theory and experiment might be improved. In Sec. 2 of this paper Fawcett's calculation is extended to include the determination of the optical matrix elements. A general procedure is set up to compute the absorption for an arbitrary band structure and used here to take account of the warped nature of the valence band. In Sec. 3 a detailed comparison is made of the differential absorption data obtained at 77°K and computed results based on known band gaps and cyclotron-resonance data using our extension of Fawcett's theory. For comparison, results using Kane's theory are presented. A similar comparison between theory and experimental data is made for the total absorption. As anticipated, the use of Fawcett's theory improves the fit of theory to experiment, but significant differences remain. Possible origins of the discrepancies are discussed briefly in Sec. 4.

¹ R. Newman and W. W. Tyler, *Phys. Rev.* **105**, 885 (1957).

² H. B. Briggs and R. C. Fletcher, *Phys. Rev.* **91**, 1342 (1953).

³ W. Kaiser, R. J. Collins, and H. Y. Fan, *Phys. Rev.* **91**, 1380 (1953).

⁴ Where the heavy-mass band $\equiv 1$, light-mass band $\equiv 2$, and split-off band $\equiv 3$.

⁵ A. H. Kahn, *Phys. Rev.* **97**, 1947 (1955).

⁶ E. O. Kane, *J. Phys. Chem. Solids* **1**, 82 (1956).

⁷ M. A. C. S. Brown and E. G. S. Paige, *Phys. Letters* **7**, 1 (1961).

⁸ A. C. Baynham and E. G. S. Paige, *Phys. Letters* **6**, 7 (1963).

⁹ W. Fawcett, *Proc. Phys. Soc. (London)* **85**, 931 (1965).

II. THEORETICAL EVALUATION OF THE ABSORPTION

A. Determination of the Band Structure and Optical Matrix Elements

The method of calculating the valence-band structure by including exactly the $\mathbf{k} \cdot \mathbf{p}$ interactions between the valence band and the nearest three conduction bands has been discussed in detail by Fawcett.⁹ This procedure leads to an 18×18 matrix containing as parameters three momentum matrix elements P , Q , R , representing the interaction between the valence band and the three conduction bands. P describes the interaction between the nearest conduction band Γ_2^- and the valence band Γ_{25}^+ , while Q and R describe, respectively, the interaction of the valence band with the two conduction bands Γ_{15}^- , Γ_{12}^- . Here the bands are labeled according to the representation of the cubic single group according to which they transform. The energy gaps at $\mathbf{k}=0$ between the interacting bands and the $\mathbf{k}=0$ spin-orbit splittings of the valence band and the Γ_{15}^- band also appear in the matrix. As discussed below, most of these parameters are available from experimental data.

In order to evaluate the optical absorption we require the matrix elements of $\mathbf{A} \cdot \mathbf{p}$ (where \mathbf{A} is the vector potential and \mathbf{p} the momentum operator) between valence-band states at a general point in \mathbf{k} space. Within the framework of the present 4-band model, the wave function of a valence-band state (i, α) at some point \mathbf{k} is of the form

$$\sum_{j\beta} a_{i\alpha, j\beta}(\mathbf{k}) \phi_{j\beta},$$

where the $\phi_{j\beta}$ are the basis functions, and the $a_{i\alpha, j\beta}$ the eigenvectors of the 18×18 matrix. Here the Roman subscripts label the band while the Greek subscripts label the twofold degenerate states within the band. The optical matrix element between two valence-band states $i\alpha$, $j\beta$ is then given by

$$\sum_{m\gamma n\delta} a_{i\alpha, m\gamma}^*(\mathbf{k}) a_{j\beta, n\delta}(\mathbf{k}) \mathbf{A} \cdot \langle \phi_{m\gamma} | \mathbf{p} | \phi_{n\delta} \rangle,$$

where $\mathbf{A} \cdot \langle \phi_{m\gamma} | \mathbf{p} | \phi_{n\delta} \rangle$ is the matrix element of $\mathbf{A} \cdot \mathbf{p}$ between the basis functions $\phi_{m\gamma}$ and $\phi_{n\delta}$ and is obtained directly from the 18×18 $\mathbf{k} \cdot \mathbf{p}$ matrix on replacing \mathbf{k} by \mathbf{A} .

B. Computation of the Absorption Coefficient for a General Band Structure

It is known from the theories of Kane and Fawcett that the predicted valence-band structure is complicated by warping and nonparabolicity. In order to include both these effects, and the detailed behavior of the matrix elements, a procedure was set up for machine computation of the absorption with a completely general band structure. Its application to the inter-valence-band transitions will now be outlined.

The contribution to the absorption coefficient K_{ij} , due to transitions between the i th and j th bands, is

$$K_{ij}(h\omega) = \sum_{\mathbf{k}} \frac{8\pi^2 e^2}{V m^2 c \omega n^2} \left| \frac{\mathbf{A} \cdot \mathbf{p}(\mathbf{k})}{A} \right|_{ij}^2 \times [f_i(\mathbf{k}) - f_j(\mathbf{k})] \delta(\omega - \omega_{ij}). \quad (1)$$

Here $h\omega$ is the photon energy, $f_i(\mathbf{k})$ is the occupancy of the state at \mathbf{k} in the i th band, $h\omega_{ij}$ is the energy difference between bands i and j , n is the refractive index, and V is the volume of the crystal. Other symbols have their usual meaning. The summation extends over all \mathbf{k} states in the Brillouin zone. The twofold degeneracy of the initial state has been included explicitly in Eq. (1); the twofold degeneracy of the final state is implicit in $|\mathbf{A} \cdot \mathbf{p}(\mathbf{k})/A|_{ij}^2$, the sum of the squares of the optical matrix elements between a state in band i and the two final states in band j . We assume the material to be nondegenerate, taking $f_i(\mathbf{k}) = \exp(\epsilon_F/k_B T) \times \exp[-\epsilon_i(\mathbf{k})/k_B T]$, where ϵ_F is the Fermi energy, $\epsilon_i(\mathbf{k})$ is the energy of the state \mathbf{k} in the i th band, k_B is the Boltzmann constant, and T is the absolute temperature.

The necessity of computing the absorption for every state in \mathbf{k} space within the Brillouin zone is circumvented by the following expedients:

(i) The summation is restricted to a cubic region surrounding $\mathbf{k}=0$ and occupying approximately 1/1000 of the zone. This introduces negligible error for nondegenerate material at not too high a temperature. (ii) The eigenvalues and eigenvectors are evaluated only for those points in \mathbf{k} space within 1/48 of this cubic volume (Fig. 1). This reduction is made possible by the symmetry of the germanium structure. The weighting of points in the interior of the sampling region is then 48; the weighting factors of the points on the surface have been given by Brust.¹⁰ Matrix elements are computed with \mathbf{A} directed along the $[100]$, $[010]$, and $[001]$ directions, the resultant absorption summed and divided by 3. (iii) Within this reduced volume the contribution to the absorption is calculated at each point on a cubic array in \mathbf{k} space. The mesh of the array (Δk) is treated as an adjustable parameter. Each point in this coarse-grained \mathbf{k} space is treated as representative

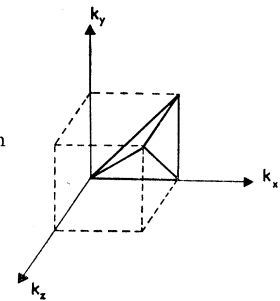


FIG. 1. The reduced zone used in the \mathbf{k} -space summation.

¹⁰ D. Brust, Phys. Rev. 134, A1337 (1964).

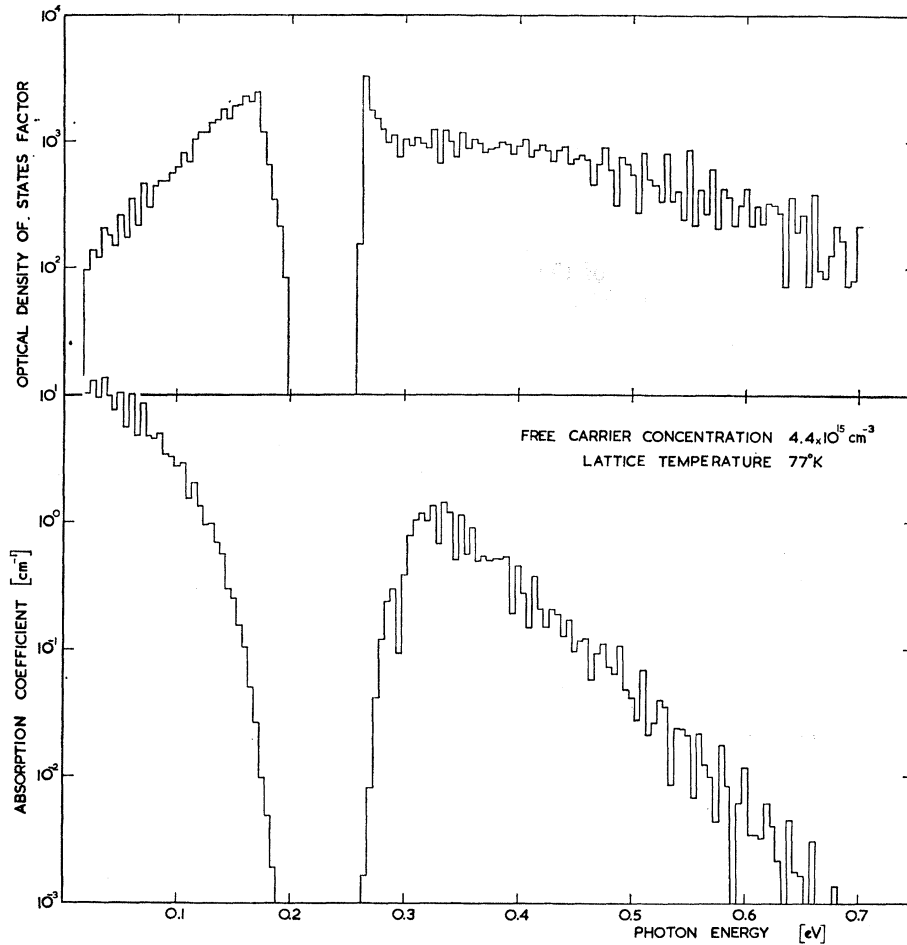


FIG. 2. Computed absorption and density-of-states histograms as a function of photon energy.

of the volume $(\Delta k)^3$; its contribution is multiplied by the number of states in $(\Delta k)^3$, $V(\Delta k/2\pi)^3$.

Contributions to K_{ij} are accumulated in a histogram of K as a function of photon energy and a mean value centered on a particular photon energy $\hbar\omega_0$ is calculated. In general this is given by

$$\bar{K}_{ij}(\hbar\omega_0) = \frac{1}{\Delta(\hbar\omega_0)} \int_{\hbar\omega_0 - \frac{1}{2}\Delta(\hbar\omega_0)}^{\hbar\omega_0 + \frac{1}{2}\Delta(\hbar\omega_0)} d(\hbar\omega) K_{ij}(\hbar\omega), \quad (2)$$

but in our procedure the histogram step $\Delta(\hbar\omega)$ is made small (typically 0.005 eV) so that it may be assumed that K_{ij} shows little dependence on energy in this range. Then $\bar{K}_{ij}(\hbar\omega_0)$ is found by dividing the summed contribution to K within each interval of the histogram by $\Delta(\hbar\omega)$.

Finally, both the Fermi energy and $(\Delta k)^3$ are eliminated from Eq. (1) by noting that the free-carrier concentration P can be written as

$$P = 2 \left(\frac{\Delta k}{2\pi} \right)^3 \exp\left(\frac{\epsilon_F}{k_B T} \right) \sum_i \sum_{\mathbf{g}} \exp\left(\frac{-\epsilon_i(\mathbf{g})}{k_B T} \right), \quad (3)$$

where i is summed over the three valence bands and \mathbf{g} is the allowed value of the wave vector in the coarse-grained \mathbf{k} space. Thus, the actual form of $K_{ij}(\hbar\omega)$ in Eq. (2) is

$$K_{ij}(\hbar\omega) = \frac{4\pi^2 P e^2}{3c n m^2 \hbar \omega} \sum_{\mathbf{g}} [|p_x(\mathbf{g})|_{ij}^2 + |p_y(\mathbf{g})|_{ij}^2 + |p_z(\mathbf{g})|_{ij}^2] \times \frac{[\exp\{-\epsilon_i(\mathbf{g})/k_B T\} - \exp\{-\epsilon_j(\mathbf{g})/k_B T\}]}{\sum_i \sum_{\mathbf{g}} \exp[-\epsilon_i(\mathbf{g})/k_B T]} \times \delta(\hbar\omega - \hbar\omega_{ij}). \quad (4)$$

The histogram obtained by this means showed significant fluctuations even when a total of approximately 50 000 points were being sampled. Figure 2 shows such a histogram for the total absorption together with a histogram of the density of states. There is experimental evidence¹¹ that appreciable temperature-dependent lifetime broadening occurs for transitions in-

¹¹ A. C. Baynham and E. G. S. Paige, in *Proceedings of the 7th International Conference on the Physics of Semiconductors, Paris, 1964* (Dunod Cie, Paris, 1964), p. 149.

volving band 3. Empirically it is found that this could be represented best by Gaussian broadening of 0.0086 eV at 77°K and 0.0087 eV at 93°K. Similar broadening effects, though less strong, are operative in the (1-2) transition. The result of broadening the computed absorption data is shown in Fig. 4. As a consequence of broadening, transitions involving band 3 have become a smooth function of energy.

The computation of the differential absorption was effected by calculating the total absorption at the two extremes of temperature, broadening each, and taking their difference. Spurious oscillations due to fluctuations in the sampled density of states were present at large photon energies. These were particularly noticeable in the differential absorption spectrum but could be rendered negligible by reducing Δk . The final value $\Delta k = 2.2 \times 10^{-3}$ a.u. was chosen such that no significant change was produced in the computed absorption on further reduction of Δk .

III. COMPARISON OF THEORY AND EXPERIMENT

Previous comparisons of theory and experiment have successfully accounted for the major structural features in the total absorption. In the present work we take this comparison further, not only making quantitative comparison with the total absorption spectrum, but also making the more demanding comparison with the differential absorption spectrum. Our primary concern, then, is with the differential absorption.

The comparison will be made with data at 77°K. This choice of temperature is a compromise. It is advantageous to go to low temperatures because phonon-induced effects are then minimized; phonon-assisted indirect transitions and the associated lifetime broadening become less important. Also temperatures are approached at which the band parameters have been determined. However, at very low temperatures free-carrier freeze-out occurs. The localized carriers make a significant contribution to the absorption which, because of the range of \mathbf{k} vectors in the Fourier transform of the localized impurity state, extends over the same spectral range as the free-carrier absorption at about 100°K. The choice of 77°K was made because lifetime broadening is estimated to be close to its minimum value,¹¹ while indirect transitions contribute less than 10% to the total absorption and 15% to the differential absorption in the spectral range of interest. Cyclotron-resonance measurements have been made up to 100°K on *p*-type germanium.¹² The importance of freeze-out is dependent on impurity concentration and compensation as well as temperature. For the 4- Ω cm samples

used in obtaining the differential absorption at 77°K the percentage of carriers frozen out is estimated to be 8%, and at 93°K to be 5%, while the actual reduction in the absorption produced by freeze-out is substantially less because of the localized impurity contribution discussed above.

The differential absorption was determined from measurements of the change in intensity of transmitted light produced by a small increase in lattice temperature. Chopped monochromatic radiation is phase-sensitively detected after passing through the germanium specimen. This signal is amplified, so that when integrated it is exactly equal to a reference voltage V . An oscilloscope, connected differentially between the integrated signal and the reference standard, detects the out-of-balance signal S occurring when the specimen is heated by a 2-sec current pulse. The ratio S/V defines the change of absorption, which, unlike conventional measurements, does not require a knowledge of reflection loss or incident intensity.

More structure is evident in the differential absorption than in the total absorption. It arises primarily from the change in energy distribution of holes with temperature. This is most clearly seen from the (1-3) transitions occurring at photon energies above 0.295 eV; the rise in temperature depletes the carrier concentration at low energies and raises it at high energies. Immediately below 0.295 eV a peak due to (2-3) transitions occurs, the negative differential absorption being masked by the effects of lifetime broadening. This experimental data will now be compared with theory.

As indicated in Sec. II, several parameters enter the theory, some of which are well known, others are not known accurately, although, by reference to cyclotron-resonance data, limits can be put on the extent to which they can be varied. In fitting theory to the experimental differential absorption, parameters have been chosen subject to the constraint that they remain consistent with cyclotron-resonance data. The parameters finally selected are listed below:

$$\begin{aligned} E(\Gamma_2^-) &= 0.89 \text{ eV}, & E(\Gamma_{15}^-) &= 3.2 \text{ eV}, & E(\Gamma_{12}^-) &= 6.0 \text{ eV} \\ P &= 0.691 \text{ a.u.}, & Q &= 0.584 \text{ a.u.}, & R &= 0.353 \text{ a.u.}, \\ \Delta(\Gamma_{25}^+) &= 0.295 \text{ eV}, & \Delta(\Gamma_{15}^-) &= 0, \end{aligned}$$

where $E(i)$ is the energy gap at $\mathbf{k}=0$ between the highest energy valence band and the i th band, and $\Delta(i)$ is the spin-orbit splitting of the i th band.

In selecting these parameters, $E(\Gamma_2^-)$ ¹³ and $\Delta(\Gamma_{25}^+)$ ⁸ were regarded as fixed. Variation of $\Delta(\Gamma_{15}^-)$ between zero and an acceptable upper limit had a negligible effect on the absorption. The remaining parameters, P , Q , R , $E(\Gamma_{15}^-)$, and $E(\Gamma_{12}^-)$, are related to the

¹² G. B. Dresselhaus, A. F. Kip, and C. Kittel, *Phys. Rev.* **98**, 368 (1955); B. W. Levinger and D. R. Frankl, *J. Phys. Chem. Solids* **20**, 281 (1961); D. M. S. Bagguley, R. A. Stradling, and J. S. S. Whiting, *Proc. Roy. Soc. (London)* **A262**, 340 (1961).

¹³ G. G. Macfarlane, T. P. McLean, J. E. Quarrington, and V. Roberts, *Proc. Phys. Soc. (London)* **71**, 863 (1958).

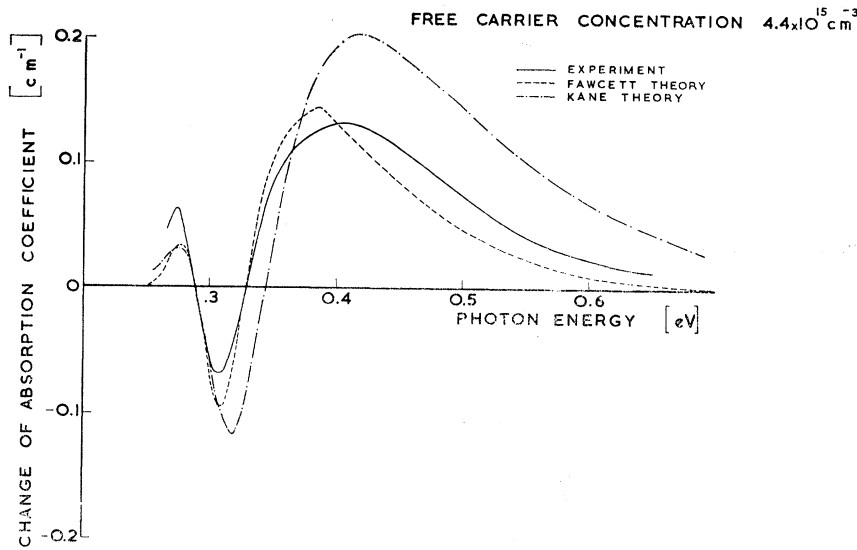


FIG. 3. Comparison of the theoretical and experimental change of absorption introduced by a 15.5°K increment of lattice temperature from 77°K.

effective-mass constants A , B , and C ¹² by

$$A = \frac{\hbar^2}{2m} + \frac{1}{3} \left(\frac{P^2}{E(\Gamma_2^-)} + \frac{2Q^2}{E(\Gamma_{15}^-)} + \frac{2R^2}{E(\Gamma_{12}^-)} \right),$$

$$B = \frac{1}{3} \left(\frac{P^2}{E(\Gamma_2^-)} - \frac{Q^2}{E(\Gamma_{15}^-)} + \frac{2R^2}{E(\Gamma_{12}^-)} \right),$$

$$C = \frac{1}{3} \left(\frac{2P^2}{E(\Gamma_2^-)} + \frac{R^2}{E(\Gamma_{12}^-)} \right) \left(\frac{2Q^2}{E(\Gamma_{15}^-)} - \frac{3R^2}{E(\Gamma_{12}^-)} \right).$$

The parameters P , Q , and R are not fixed by these equations because of the spread in the experimental values of A , B , C ,¹² and $E(\Gamma_{15}^-)$.¹⁴ Herman¹⁵ has estimated that $E(\Gamma_{12}^-)$ is about 10 eV. Fitting was attempted by varying $E(\Gamma_{12}^-)$ between 6 and 12 eV and $E(\Gamma_{15}^-)$ within the range of experimental values. P , Q , and R were varied so as to be consistent with these values and the range of experimental values of A , B , and C . The sensitivity of the differential absorption to the permitted variation was not strong; for example, the extremes in amplitude of the positive (1-3) transition peak were -5% to +15% about the value predicted from the selected parameters.

The theoretical curve computed using the listed parameters is plotted in Fig. 3. It will be seen that the positioning of the structure (maxima, minima, and points of zero differential absorption) is in good agreement with the experimental data. However, the magnitude does not always compare so favorably. To illustrate the effect on the computed absorption of the change from the perturbation $\mathbf{k} \cdot \mathbf{p}$ calculation to the exact $\mathbf{k} \cdot \mathbf{p}$ treatment, the differential absorption com-

puted from Kane's theory is also shown in Fig. 3. The same parameters, or their equivalent, were used and the same computational procedure followed. The sensitivity to variation of parameters was no greater than that of the exact calculation. We comment on these results below.

Figure 4 shows plots of the total absorption at 77°K computed using the exact and the perturbation $\mathbf{k} \cdot \mathbf{p}$ theory. For comparison, experimental data¹⁶ are presented. There has been no attempt to fit the theoretical and experimental curves for the total absorption, the parameters used in the computation being the same as those listed above. The position of the (1-3) peak is accurately predicted by the exact $\mathbf{k} \cdot \mathbf{p}$ theory, though the magnitude of the absorption in the wings of the peak is underestimated (notice that the vertical scale is logarithmic). The perturbation theory shows a large over-estimate at high photon energies. This was originally noted by Kane⁶ and, in fact, led him to suggest that a more accurate calculation, such as we have presented, was required.

The comparison, of both the total (Fig. 4) and the differential absorption (Fig. 3), shows that there are discrepancies of up to approximately a factor of 2 between experiment and perturbation theory. Adjustment of parameters consistent with known band-structure data and inclusion of estimated changes in free-carrier concentration do not significantly improve the agreement. In contrast, Figs. 3 and 4 show that discrepancies between the exact $\mathbf{k} \cdot \mathbf{p}$ theory and experiment are typically only 25% in the region of the (1-3) transition, and in good agreement with regard to position of structure. With the experimental data available it is difficult to press this comparison further for the (1-3) transitions, since we should need to know accurately the absorption of neutral acceptors as well as

¹⁴ M. Cardona and G. Harbeke, *J. Appl. Phys.* **34**, 813 (1963); J. Tauc and A. Abraham, *J. Phys. Chem. Solids* **20**, 190 (1961); M. Cardona, *ibid.* **24**, 1543 (1963).

¹⁵ F. Herman, in *Proceedings of the 7th International Conference on Physics of Semiconductors, Paris, 1964* (Dunod Cie, Paris, 1964), p. 3.

¹⁶ W. E. Pinson and R. Bray, *Phys. Rev.* **136**, A1449 (1964).

estimate with precision the contribution of indirect transitions. The discrepancy is also approaching the experimental uncertainty in the magnitude of the absorption. In the region of the (1-2) and (2-3) transitions discrepancies of a factor of 2 remain. Indeed, there is little difference between the predictions of the exact and perturbation theories.

The main improvement between experiment and theory has been achieved in the region of (1-3) transitions. This can be traced to the increased mass of band 3 predicted by the exact $\mathbf{k}\cdot\mathbf{p}$ calculation.⁹ However, the exact theory and perturbation theory are in close agreement for bands 1 and 2 and this is reflected in the similarity of the calculated absorption spectra in the (1-2) transition region. The observable (2-3) transitions are confined to states of small \mathbf{k} where all changes in the band structure are small, and therefore negligible changes are introduced by using the exact theory in this region of the spectrum.

IV. CONCLUDING COMMENTS

In this paper we have presented a more rigorous calculation of the direct interband absorption due to free carriers than has been given before. It is based on an exact $\mathbf{k}\cdot\mathbf{p}$ interaction theory of the band structure and its extension to the optical matrix elements; it incorporates the complexity of the band structure and lifetime broadening. The results of this calculation have been fitted to the differential absorption spectrum keeping the parameters involved consistent with other known band-structure data. In the spectral region where the (1-3) transitions occur a good fit is obtained, but in the (2-3) transition region there is no significant improvement over the perturbation theory. The same is true of a comparison with the total absorption using the same parameters, but, in addition, it is seen that when (1-2) transitions occur the agreement is again no better than with perturbation theory. We conclude by briefly discussing possible origins of these remaining discrepancies between theory and experiment.

No contribution from indirect transitions has been explicitly introduced into our calculations although the existence of such transitions is implicit in the introduction of lifetime broadening. Since the discrepancy between the present theory and experiment becomes most marked at low photon energies, it is tempting to suggest that indirect transitions make a significant contribution to the absorption. However, if it is assumed that at 30μ the absorption is dominated by indirect transitions, extrapolation of the experimental data³ to wavelengths of interest here according to the Drude-Zener λ^2 law, suggests that the contribution will be insufficient to account for the discrepancy. This is corroborated by a crude estimate of the strength of the indirect transition, and also by the fact that, though indirect transitions would not be devoid of structure, the structure that would be necessary to close the gap between experiment and theory appears unrealistic.

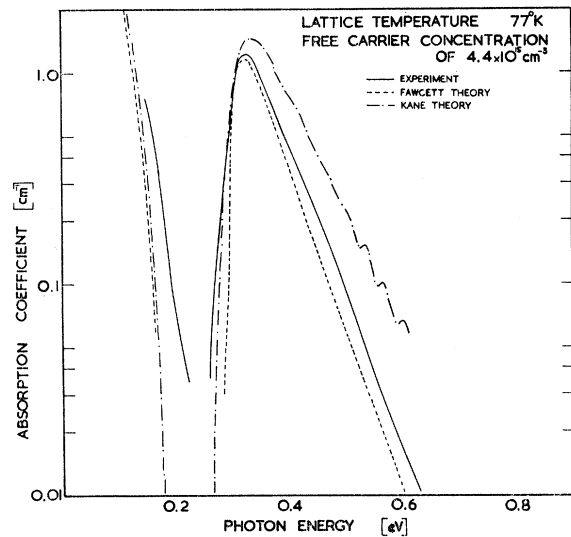


FIG. 4. Comparison of the theoretical and experimental total-absorption spectra.

Another source of discrepancy is freeze-out, which is small, and for which we have made no allowance on the grounds of the similarity of the ionization spectrum of the acceptor and the free-carrier absorption. Obviously, this is a crude approximation and will become increasing poor away from $\mathbf{k}=0$. A comparison of 77 and 4°K data would be of interest here. What evidence there is⁸ suggests that the results are very similar, though caution is necessary because of the high doping level at which these observations were made.

These comments highlight the need for a theoretical as well as an experimental investigation of the impurity and indirect-absorption spectra. A theoretical approach which abandons the rigid-lattice assumption from the outset would be desirable; it would then embody indirect phonon-assisted transitions, "lifetime broadening," as well as temperature dependence of the band structure and could be applied at temperatures where freeze-out was negligible.

Finally we remark on deficiencies in the $\mathbf{k}\cdot\mathbf{p}$ theory presented here. This theory is limited to interactions between the valence band and three other bands. With the exception of a Γ_1^+ band predicted by Herman¹⁵ to be 7.76 eV from the valence band, the remaining bands are remote in energy, while the Γ_1^+ band does not interact directly with the valence band.¹⁷ Other neglected features are the \mathbf{k} -dependent contribution to the spin-orbit interaction and also several relativistic and interband spin-orbit interactions. None of these approximations are expected to have a significant effect on the band structure near the center of the zone.

¹⁷ Recently M. Cardona and F. H. Pollak [Phys. Rev. **142**, 530 (1966)] have included extra bands in a $\mathbf{k}\cdot\mathbf{p}$ calculation of the band structure of germanium throughout the zone but did not include spin-orbit splitting. When the spin-orbit interaction was included, the magnitude of the computing problem required that only neighboring bands be taken into account. The resulting valence-band shapes then differ insignificantly from those used in the present calculation.